

## Effect of natural flours on crystallization behaviors of poly(3-hydroxybutyrate-co-3-hydroxyhexanoate)

Deepika Jonnalagadda, Takashi Kuboki

Department of Mechanical and Materials Engineering, University of Western Ontario, London, Ontario N6A 5B9, Canada

Correspondence to: T. Kuboki (E-mail: tkuboki@uwo.ca)

**ABSTRACT:** This paper investigates the effects of natural flours on the crystallization behavior of poly(3-hydroxybutyrate-co-3-hydroxyhexanoate) (PHBH). Two types of PHBH (3-hydroxyhexanoate [3HH] contents of 5.6 and 11.1 mol %) were used as polymer matrix. One of two natural flours (cellulose or wood) at 1 wt % was added to this PHBH matrix. Crystallization behaviors under nonisothermal conditions were characterized using differential scanning calorimetry (DSC), while those under isothermal conditions were characterized using DSC and polarized optical microscopy. The results suggested that both cellulose and wood flour addition enhanced crystallization of the PHBH containing 5.6 mol % of 3HH (i.e., increased crystallization peak temperature and degree of crystallinity under the nonisothermal conditions, as well as decreased crystallization half time under the isothermal conditions). Of the two flours, wood flour was found to have greater effects, due to its higher crystal nucleating ability. © 2016 Wiley Periodicals, Inc. *J. Appl. Polym. Sci.* 2016, 133, 43600.

**KEYWORDS:** biopolymers & renewable polymers; cellulose and other wood products; crystallization; differential scanning calorimetry; thermal properties

Received 22 October 2015; accepted 6 March 2016

DOI: 10.1002/app.43600

### INTRODUCTION

Polyhydroxyalkanoates (PHAs) are microbial polyesters produced by a wide range of microorganisms.<sup>1</sup> They have attracted much attention for their biodegradability with no toxic waste, their biocompatibility, and their mechanical properties being comparable to commercial nonbiodegradable plastics.<sup>2–5</sup> Poly(3-hydroxybutyrate) (PHB) is a member of the PHA family and is a linear isotactic homopolymer. PHB has a high melting temperature and tensile strength, but low degradation temperature (i.e., narrow processing temperature window) and low elongation at break due to its high degree of crystallinity.<sup>6–8</sup> For this reason, a comonomer, 3-hydroxyvalerate (3HV), was introduced into PHB, resulting in the formation of the copolymer poly(3-hydroxybutyrate-co-3-hydroxyvalerate) (PHBV).<sup>9</sup> Although this copolymerization mitigated the brittleness to some extent, the 3-hydroxybutyrate (3HB) and 3HV comonomers of PHBV are isodimorphous; i.e., these two monomers' similarity in shape and size allows their incorporation into the same crystalline lattice without distortion of lattice parameters.<sup>10–12</sup> Due to isomorphism, many of the usual benefits of copolymerization are not realized. Therefore, it was desired to copolymerize 3HB with units containing longer hydroxyalkanoic acids chains, such that the two comonomers would not fit into each other's crystalline lattice, thus avoiding isomorphism.

A longer chain comonomer, 3-hydroxyhexanoate (3HH), has been introduced into PHB, resulting in formation of the copolymer poly(3-hydroxybutyrate-co-3-hydroxyhexanoate) (PHBH).<sup>13–16</sup> PHBH displays a broad range of thermal and mechanical properties when its comonomer content is changed. Melting temperature decreases and decomposition temperature increases with the increase of 3HH content.<sup>17,18</sup> Also, elongation at break increases but modulus and strength decrease with increasing 3HH content.<sup>18,19</sup>

It has also been reported that the introduction of 3HH results in reduction of crystal growth rate and degree of crystallinity.<sup>20</sup> In addition, since PHBH is produced by a fermentation process that yields very pure material after solvent extraction from bacterial cells, the crystal nucleation density is low. This raises technical problems in melt processing such as extrusion and injection molding, where rapid crystallization is required. Slow crystallization results in long molding-cycle time, thus leading to low productivity and high energy consumption in industrial processing. In addition, a large fraction of PHBH remains amorphous due to the low degree of crystallinity and slowly undergoes secondary crystallization during storage or its service life,<sup>19</sup> which results in the change of mechanical properties over time and impacts long-term performance in practical applications. For this reason, in the past, various nucleating agents (NAs) were applied to PHBH with the goal of increasing its crystal nucleation density and crystallization rate.

**Table I.** Material information of Materials Used in this Study

Name	PHBH with 5.6 mol % of 3HH (wt %)	PHBH with 11.1 mol % of 3HH (wt %)	Cellulose flour (wt %)	Wood flour (wt %)
PHBH5.6	100			
PHBH5.6C	99		1	
PHBH5.6W	99			1
PHBH11.1		100		
PHBH11.1C		99	1	
PHBH11.1W		99		1

These NAs included boron nitride,<sup>21,22</sup> orotic acid,<sup>21</sup> thymine,<sup>22</sup> cytosine,<sup>22</sup> uracil,<sup>22</sup> L-phenylalanine,<sup>23</sup> cyclodextrin complex,<sup>24</sup> layered metal phosphates,<sup>25</sup> and cyanuric acid.<sup>26</sup>

In order to reinforce polymers, natural fibers or flours have been used as a replacement for inorganic fibers or fillers. Their attractive features are low density, low cost, recyclability, renewability, nonabrasiveness, and thermal recyclability. When natural fibers or flours are incorporated into PHBH, the composite materials are renewable and bio-degradable, thus allowing the production of sustainable products. However, only a few studies have reported on and described the crystallization behavior of biocomposite materials resulting from the addition of natural fibers or flours to PHBH. It was reported that flax fibers were used as reinforcements and that the fibers with modified surface were found to have a nucleation effect on crystallization.<sup>27</sup> Recently, porous cellulose used as a reinforcement was found to accelerate the crystallization of PHBH.<sup>28</sup>

Wood and cellulose pulp are the most prevalent natural fibers or flours due to their availability, and they have been used to reinforce various polymers.<sup>29–33</sup> However, to the authors' knowledge, their applications to PHBH have not been reported in literature yet. It is imperative to understand whether wood and cellulose fiber/flour can act as crystal nucleating agents to reduce processing time as well as produce small and uniform spherulites of PHBH. In this context, this study investigated the effects of wood and cellulose flours on nonisothermal and isothermal crystallization behaviors of two types of PHBH, varying in 3HH content.

## EXPERIMENTAL

### Materials

Two types of PHBH, supplied by Kaneka Corporation, were used as polymer matrix. The PHBH were different in 3HH content and molecular weight: one had a 3HH molar content of 5.6% and a molecular weight of 555,000 g/mol; the other had a 3HH molar content of 11.1% and a molecular weight of 622,000 g/mol. Two types of natural flour were used: cellulose flour, supplied by CreaFill Fibers Corporation; and wood flour, supplied by American Wood Fibers.

PHBH and natural flours were dried in a convection oven at, respectively, 80 °C for 3 h and 110 °C for 12 h before compounding. PHBH and natural flours were compounded using a mini-twin-screw extruder (HAAKE MiniLab) at 100 rpm for 10

min. The barrel temperature was set to 150 °C. The two types of PHBH (i.e., PHBH with 3HH contents of 5.6 and 11.1 mol %) were combined with 1 wt % of one of the two natural flours (i.e., cellulose flour or wood flour) or without flour to prepare six materials. Information on the materials is summarized in Table I. In the rest of the text, the names given in the table (i.e., PHBH5.6, PHBH5.6C, PHBH5.6W, PHBH11.1, PHBH11.1C, and PHBH11.1W) are used to refer to the materials.

### Differential Scanning Calorimetry (DSC)

Nonisothermal and isothermal crystallization behaviours of the materials were characterized under nitrogen flow using DSC (Q200, TA Instruments). Indium was used for temperature and heat-of-fusion calibration. Mass of samples used for the DSC measurements was between 7 and 8 mg. For nonisothermal crystallization, a sample was heated to 190 °C at 10 °C/min and held at that temperature for 3 minutes to erase the thermal history. Then, the sample was cooled to −40 °C at 5 °C/min and held at that temperature for 3 min. Lastly, the sample was reheated to 190 at 5 °C/min. The same experimental procedure was repeated with the rate of 10 °C/min instead of 5 °C/min as the cooling and reheating rate. It is noted that the cooling rates of 5 °C/min and 10 °C/min are slower than those encountered in extrusion and injection molding processes.

For isothermal crystallization, a sample was heated to 190 °C at 10 °C/min and held at that temperature for 3 min to erase the thermal history. Then, the sample was cooled to the isothermal temperature of 50 °C at 50 °C/min and held at that temperature until crystallization was completed. The same experimental procedure was repeated for the isothermal temperatures of 70, 90, and 100 °C.

### Polarized Optical Microscopy (POM)

Spherulitic morphology was examined under the same thermal histories as those of DSC isothermal crystallization using a polarized optical microscope (Laborlux 11 POL, Leitz) equipped with a digital camera. A thin sample slice was situated on top of a sapphire disc and placed inside a Linkam TS1500 heating stage (Linkam Scientific Instruments), which was then controlled by a Linkam TMS94 temperature controller (Linkam Scientific Instruments) to heat the sample to 190 °C at 10 °C/min, hold it at 190 °C for 3 min, and then cool it at 50 °C/min to the desired temperature (either 70 or 90 °C) for isothermal crystallization. Imaging analysis software (Infinity Analyze, Lumenera Corporation) was used to capture images and quantify spherulite radius magnitudes during spherulite growth before impingement. A slope of spherulitic radius  $R$  versus time after isothermal onset  $t$  was used to determine spherulite linear radius growth rate  $G$  as in  $G = dR/dt$ .

## RESULTS AND DISCUSSION

### Nonisothermal Crystallization

Figure 1 shows nonisothermal DSC cooling curves [Figure 1(a)] and subsequent heating curves [Figure 1(b)] of neat PHBH5.6 and neat PHBH11.1, as well as of PHBH5.6 and PHBH11.1 containing 1 wt % of cellulose or wood flour, subjected to the rate of 5 °C/min. Table II summarizes thermal properties of the materials estimated from the DSC curves, including glass transition temperature ( $T_g$ ), crystallization peak temperature ( $T_c$ ),

cold crystallization peak temperature ( $T_{cc}$ ), melting peak temperatures ( $T_{m1}$ ,  $T_{m2}$ ), enthalpy of crystallization ( $\Delta H_c$ ), enthalpy of cold crystallization ( $\Delta H_{cc}$ ), enthalpy of fusion ( $\Delta H_m$ ) and degree of crystallinity ( $X_c$ ). Degree of crystallinity ( $X_c$ ) was computed as follows:

$$X_c = \frac{\Delta H_m - \Delta H_{cc}}{\Delta H_m^0} \times 100\% \quad (1)$$

where the enthalpy of an infinitely large crystal of PHB was taken to be  $\Delta H_m^0 = 146 \text{ J g}^{-1}$ .<sup>34</sup> It is noted that when enthalpy of fusion ( $\Delta H_m$ ) is calculated, the heat flow was scaled by  $T_m^0/T$  to compensate for lower entropy of fusion of thin crystals,<sup>35</sup> where  $T_m^0$  (K) is the equilibrium melting temperature of PHB ( $=188 \text{ }^\circ\text{C}$ <sup>36</sup>) and  $T$  (K) is temperature.

Double melting behavior was observed in all materials. The first melting peak  $T_{m1}$  originates from the melting of the crystals formed originally, while the second melting peak  $T_{m2}$  emerges from the melting of the crystals formed due to recrystallization during the heating process.<sup>37–41</sup> In agreement with findings reported in the past,<sup>37</sup> melting peak temperatures  $T_{m1}$  and  $T_{m2}$  and degree of crystallinity decreased with the increase of 3HH content (in this study, from 5.6 to 11.1 mol %); the 3HH comonomer suppressed crystallization and disturbed the poly(3HB)-type crystal lattice.

It is evident from the cooling curves [Figure 1(a)] that both PHBH5.6C and PHBH5.6W had a higher  $T_c$  and larger enthalpy of crystallization than did neat PHBH5.6. This finding indicates that the addition of natural flours increased the crystallization peak temperature of PHBH5.6. The increase in  $T_c$  of PHBH5.6 as a result of wood flour (about a  $20 \text{ }^\circ\text{C}$  increase) can be seen to be greater than that as a result of cellulose flour (about a  $12 \text{ }^\circ\text{C}$  increase). In PHBH11.1-based materials, however, neat PHBH11.1 did not show a crystallization peak and the addition of cellulose and wood flour could not generate a crystallization peak.

In the subsequent heating process [Figure 1(b)], a cold crystallization peak with large enthalpy ( $\Delta H_{cc} = 35.0 \text{ J/g}$ ) was observed in neat PHBH5.6. However, the addition of cellulose flour (PHBH5.6C) significantly reduced enthalpy of cold crystallization ( $\Delta H_{cc} = 1.52 \text{ J/g}$ ), which is indicated by the arrow in the figure. Furthermore, the addition of wood flour (PHBH5.6W) eliminated enthalpy of cold crystallization. This difference between neat PHBH5.6 and natural flour-containing PHBH5.6 may be the result of a larger amount of PHBH having been crystallized during the cooling process due to cellulose and wood flour addition, such that, during the heating process, the PHBH samples containing natural flours had less amorphous polymer that could transform to crystals. In the case of the wood flour-containing PHBH, for example, practically all of the crystallizable amorphous polymer in PHBH had already crystallized in the cooling process, resulting in negligible crystallization during the heating process.

Moreover, cellulose and wood flour addition increased the degree of crystallinity of PHBH5.6 from 18.6% to, respectively, 40.4 and 41.6%. Additionally, in PHBH5.6, cellulose and wood flour addition increased melting peak temperature  $T_{m1}$ , possibly

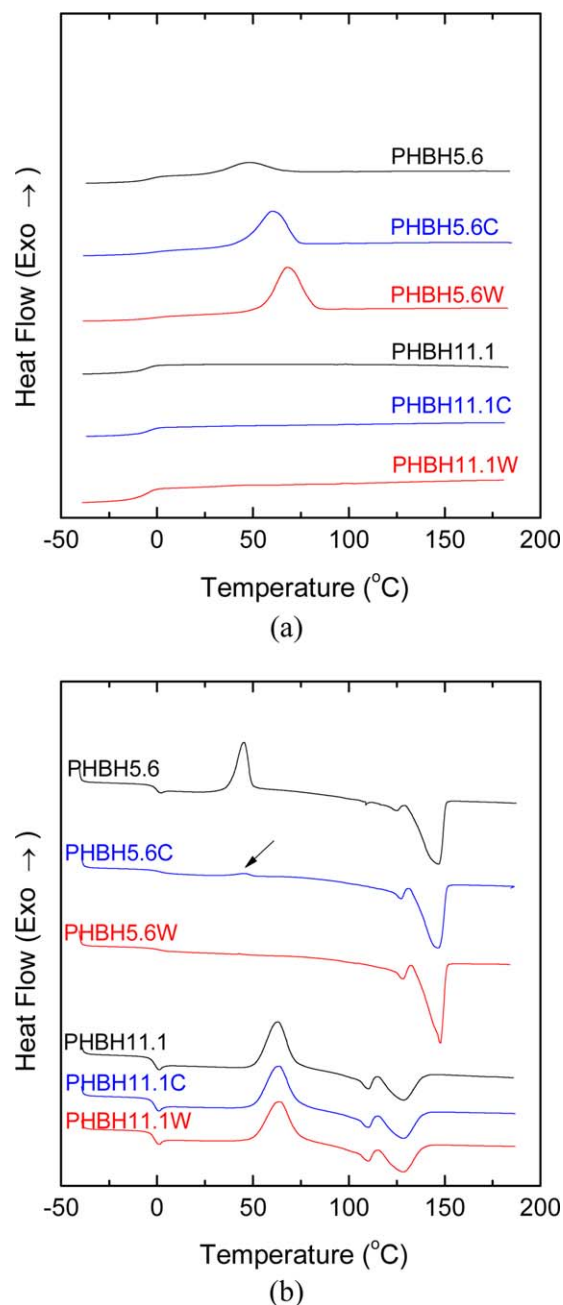


**Figure 1.** DSC curves at  $5 \text{ }^\circ\text{C}/\text{min}$  for PHBH5.6- and PHBH11.1-based materials: (a) cooling scans and (b) subsequent heating scans, where the arrow indicates enthalpy of cold crystallization of PHBH5.6C. [Color figure can be viewed in the online issue, which is available at [wileyonlinelibrary.com](http://wileyonlinelibrary.com).]

as a result of natural flours encouraging formation of greater lamellar crystal thickness, from  $125.7 \text{ }^\circ\text{C}$  to, respectively,  $127.5 \text{ }^\circ\text{C}$  and  $129.2 \text{ }^\circ\text{C}$ , but little changed  $T_{m2}$ . In contrast, all three PHBH11.1-based materials (PHBH11.1, PHBH11.1C, and PHBH11.1W) showed similar enthalpy for cold crystallization ( $\Delta H_{cc} \approx 37 \text{ J/g}$ ), had similar melting peak temperatures  $T_{m1}$  and  $T_{m2}$ , and had low degrees of crystallinity.

Figure 2 shows the DSC cooling curves [Figure 2(a)] and subsequent heating curves [Figure 2(b)] at the rate of  $10 \text{ }^\circ\text{C}/\text{min}$ , and

**Table II.** Nonisothermal Crystallization Data for Cooling and Heating Rates of 5 °C/min

Material	$T_g$ (°C)	$T_c$ (°C)	$T_{cc}$ (°C)	$T_{m1}$ (°C)	$T_{m2}$ (°C)	$\Delta H_c$ (J/g)	$\Delta H_{cc}$ (J/g)	$\Delta H_m$ (J/g)	$X_c$ (%)
PHBH5.6	-0.3	48.1	46.2	125.7	147.7	19.6	35.0	62.2	18.6
PHBH5.6C	1.0	60.1	45.2	127.5	146.7	47.8	1.52	60.5	40.4
PHBH5.6W	1.9	68.2	N.P.	129.2	148.7	55.6	0	60.7	41.6
PHBH11.1	-2.0	N.P.	63.2	110.4	128.5	0	37.4	43.7	4.3
PHBH11.1C	-1.8	N.P.	63.6	110.3	128.5	0	36.6	46.4	6.7
PHBH11.1W	-1.9	N.P.	63.9	110.3	128.5	0	36.5	46.7	7.0

N.P.: no peak.

Table III summarizes thermal properties of the materials measured from these DSC curves. In the cooling process [Figure 2(a)], the addition of natural flours had effects on PHBH5.6 similar to those exhibited when subjected to the 5 °C/min cooling rate; namely, the addition of natural flours increased crystallization peak temperature and enthalpy of crystallization of neat PHBH5.6. However, effectiveness decreased with the increase of cooling rate from 5 to 10 °C/min (specifically, at the rate of 10 °C/min, cellulose and wood flours increased crystallization peak temperature by about 4 and 9 °C, respectively, as opposed to 12 and 20 °C, respectively, as was observed at the rate of 5 °C/min). On the other hand, none of the PHBH11.1-based materials showed a crystallization peak, as was also the case when the materials were subjected to the 5 °C/min cooling rate. In the heating process [Figure 2(b)], addition of natural flours again reduced enthalpy of cold crystallization of neat PHBH5.6 but, unlike at the rate of 5 °C/min, addition of wood flour could not eliminate cold crystallization. With the increase of heating rate from 5 to 10 °C/min, the degree of crystallinity of PHBH5.6-based materials was decreased. However, similar to the cases with the rate of 5 °C/min, heating with the rate of 10 °C/min showed that addition of natural flours increased the degree of crystallinity of neat PHBH5.6. Furthermore, addition of natural flour was more effective at increasing degree of crystallinity of PHBH5.6 at the rate of 10 °C/min than that at 5 °C/min (specifically, at 10 °C/min, cellulose and wood flour addition increased the degree of crystallinity of PHBH5.6 by 3.00 and 5.11 times, respectively; whereas, at 5 °C/min, the increase was by 2.17 and 2.24 times, respectively). In PHBH11.1-based materials, neat PHBH11.1 showed only a small enthalpy of cold crystallization, but the addition of natural flours increased enthalpy of cold crystallization. This finding suggests that cellulose and wood flours acted as nucleating agents during the heating process. However, all PHBH11.1-based materials showed a low degree of crystallinity.

Glass transition temperature  $T_g$  of PHBH decreased with the increase of 3HH content, namely from 5.6 to 11.1 mol %, at both the heating rate of 5 and 10 °C/min, which suggests that long, flexible 3HH units increased the degree of segmental mobility of PHBH molecules in the amorphous phase.<sup>37</sup> Addition of cellulose and wood flours did not change  $T_g$ , thus not restricting the segmental mobility of PHBH5.6 and PHBH11.1 at 5 °C/min and 10 °C/min, except for PHBH5.6 at the heating rate of 5 °C/min (exhibiting an increase in  $T_g$ ), which further study is needed to investigate.

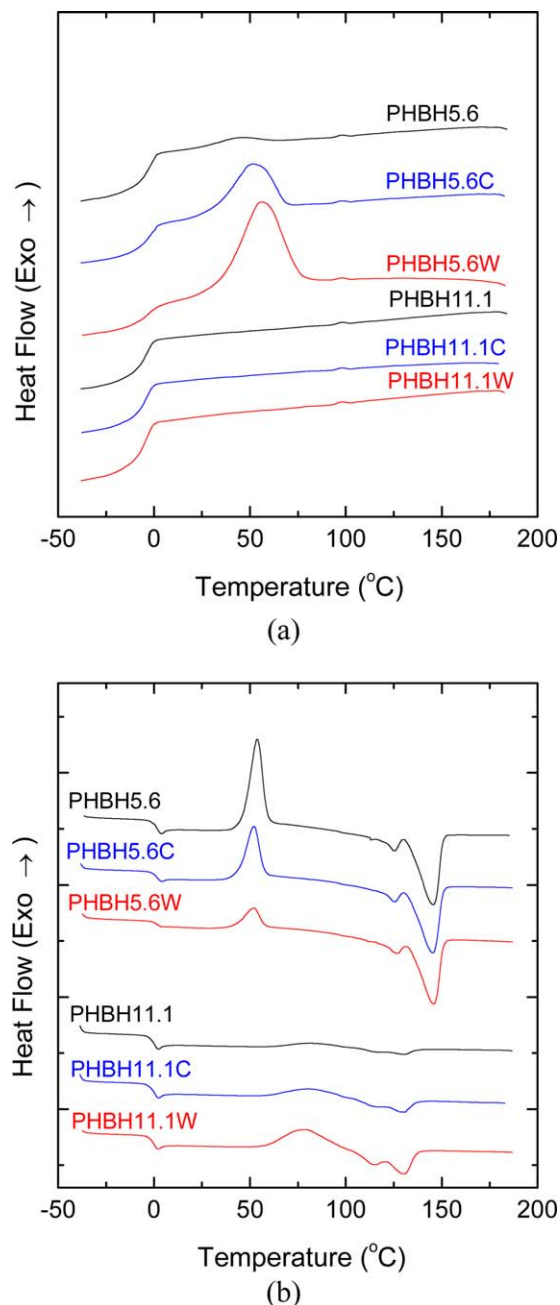


**Figure 2.** DSC curves at 10 °C/min for PHBH5.6- and PHBH11.1-based materials: (a) cooling scans and (b) subsequent heating scans. [Color figure can be viewed in the online issue, which is available at [wileyonlinelibrary.com](http://wileyonlinelibrary.com).]

**Table III.** Nonisothermal Crystallization Data for Cooling and Heating Rates of 10 °C/min

Material	$T_g$ (°C)	$T_c$ (°C)	$T_{cc}$ (°C)	$T_{m1}$ (°C)	$T_{m2}$ (°C)	$\Delta H_c$ (J/g)	$\Delta H_{cc}$ (J/g)	$\Delta H_m$ (J/g)	$X_c$ (%)
PHBH5.6	0.6	47.4	53.8	125.6	145.6	1.82	49.8	56.5	4.6
PHBH5.6C	0.9	51.8	52.1	125.7	145.3	15.2	34.8	54.9	13.8
PHBH5.6W	0.7	56.0	52.1	126.9	145.8	30.1	19.9	54.2	23.5
PHBH11.1	-0.5	N.P.	80.9	118.5	130.5	0	5.15	6.8	1.1
PHBH11.1C	-1.0	N.P.	80.1	118.3	130.0	0	10.6	14.6	2.7
PHBH11.1W	-0.9	N.P.	78.6	115.5	130.6	0	23.3	28.4	3.5

### Isothermal Crystallization

Only PHBH5.6-based materials (PHBH5.6, PHBH5.6C, and PHBH5.6W) were selected for the isothermal experiment because the results from the nonisothermal experiments indicated that the natural flours had a more significant impact on the crystallization

behavior of PHBH5.6 than on that of PHBH11.1. Isothermal DSC curves for neat PHBH5.6 and for PHBH5.6 with cellulose or wood are presented in Figure 3. At all isothermal crystallization temperatures [50 °C in Figure 3(a), 70 °C in Figure 3(b), 90 °C in Figure 3(c), and 100 °C in Figure 3(d)], addition of natural flour

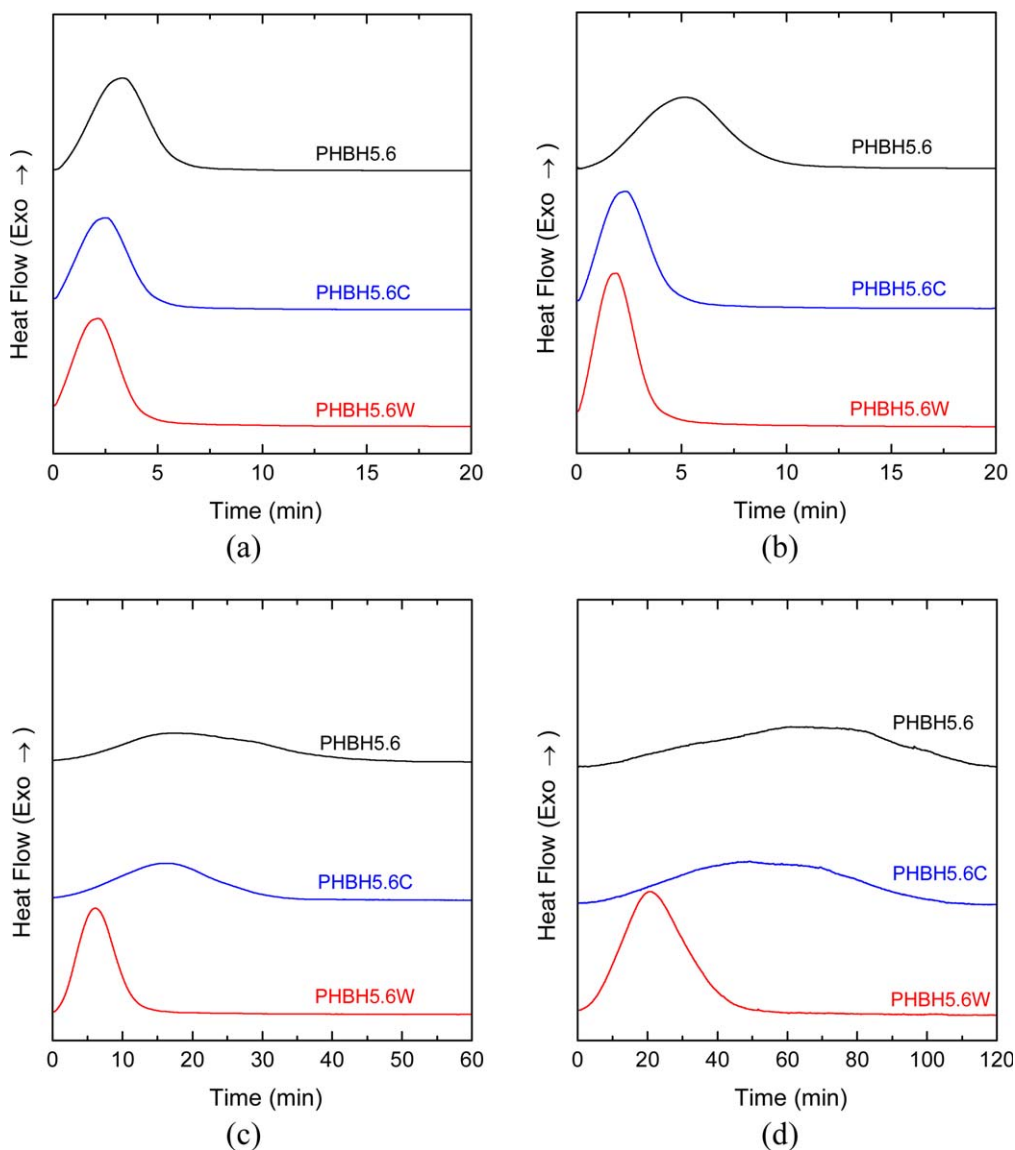


**Figure 3.** DSC curves of PHBH5.6-based materials at isothermal crystallization temperature of (a) 50, (b) 70, (c) 90, and (d) 100 °C. [Color figure can be viewed in the online issue, which is available at [wileyonlinelibrary.com](http://wileyonlinelibrary.com).]

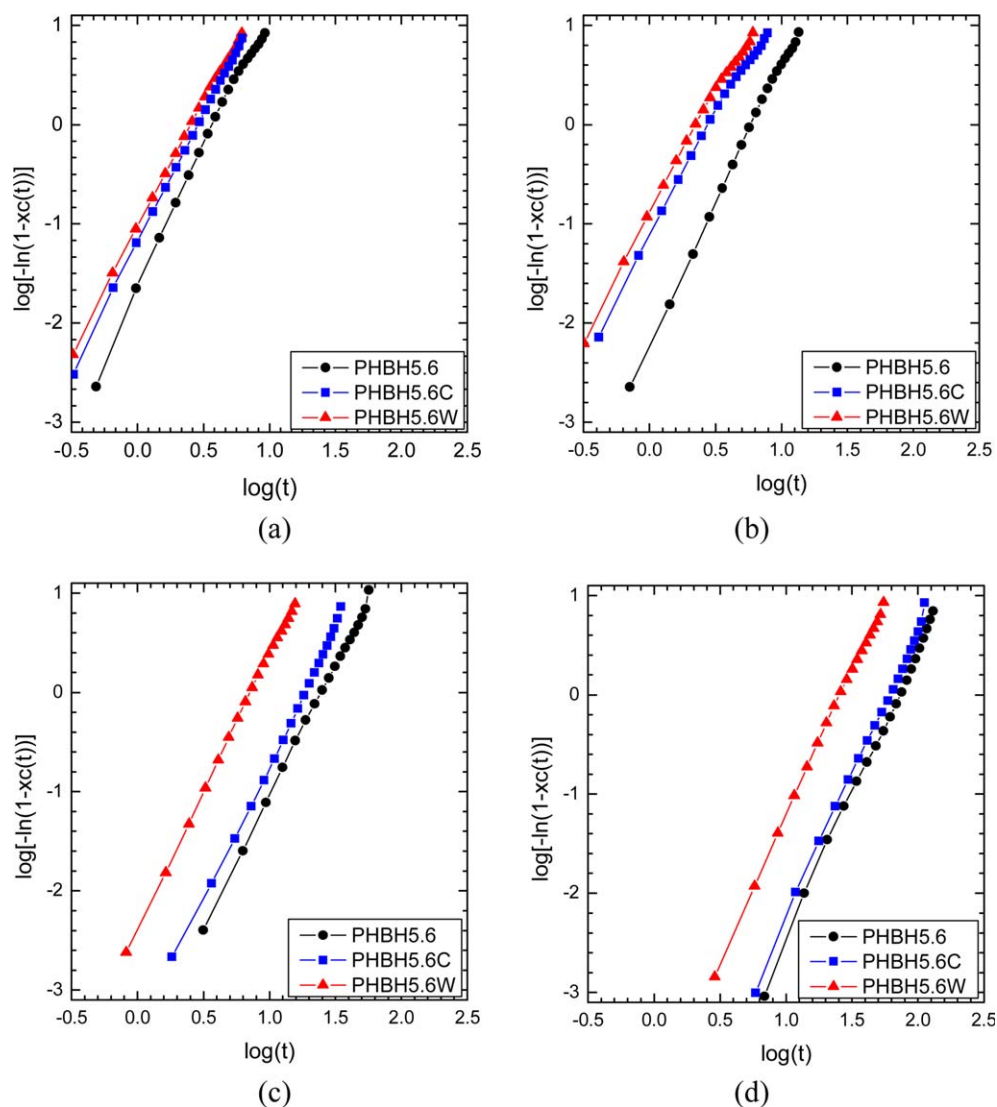


**Figure 4.** Avrami plots of PHBH5.6-based materials at isothermal crystallization temperature of (a) 50, (b) 70, (c) 90, and (d) 100 °C. [Color figure can be viewed in the online issue, which is available at [wileyonlinelibrary.com](http://wileyonlinelibrary.com).]

**Table IV.** Avrami Parameters for Isothermal Crystallization of PHBH5.6-Based Materials

Temperature (°C)	Material	$n$	$K$ (min <sup>-n</sup> )
50	PHBH5.6	2.67 (0.07)	$2.55 \times 10^{-2}$ ( $1.2 \times 10^{-3}$ )
	PHBH5.6C	2.28 (0.16)	$7.27 \times 10^{-2}$ ( $2.5 \times 10^{-3}$ )
	PHBH5.6W	2.41 (0.08)	$9.12 \times 10^{-2}$ ( $5.4 \times 10^{-3}$ )
70	PHBH5.6	2.79 (0.01)	$6.74 \times 10^{-3}$ ( $4.9 \times 10^{-4}$ )
	PHBH5.6C	2.30 (0.06)	$8.05 \times 10^{-2}$ ( $1.8 \times 10^{-3}$ )
	PHBH5.6W	2.29 (0.10)	$1.31 \times 10^{-1}$ ( $8.2 \times 10^{-3}$ )
90	PHBH5.6	2.66 (0.04)	$2.18 \times 10^{-4}$ ( $1.3 \times 10^{-5}$ )
	PHBH5.6C	2.66 (0.08)	$2.91 \times 10^{-4}$ ( $3.5 \times 10^{-5}$ )
	PHBH5.6W	2.80 (0.11)	$3.98 \times 10^{-3}$ ( $5.2 \times 10^{-4}$ )
100	PHBH5.6	2.90 (0.07)	$5.00 \times 10^{-6}$ ( $8.2 \times 10^{-7}$ )
	PHBH5.6C	2.94 (0.06)	$6.80 \times 10^{-6}$ ( $7.4 \times 10^{-7}$ )
	PHBH5.6W	2.84 (0.05)	$8.42 \times 10^{-5}$ ( $8.1 \times 10^{-6}$ )

The numbers in the parenthesis are the standard deviations ( $n = 3$ ).

**Table V.** Size of Cellulose and Wood Flours

	Length ( $\mu\text{m}$ )	Width ( $\mu\text{m}$ )
Cellulose flour	92 (46)	18 (7)
Wood flour	96 (79)	23 (13)

The numbers in the parenthesis are the standard deviations ( $n = 100$ ).

reduced time to complete crystallization; that is, natural flour accelerated the crystallization speed of PHBH5.6, with wood flour being more effective than cellulose flour.

Using the isothermal DSC curves, relative degree of crystallinity  $X_{\text{rel}}$  was calculated as follows:

$$X_{\text{rel}} = \frac{\int_0^t \frac{dH(t)}{dt} dt}{\int_0^\infty \frac{dH(t)}{dt} dt} \quad (2)$$

where the isothermal DSC curve is integrated between  $t = 0$  and  $t$ , and divided by the overall crystallization area.

The crystallization kinetics was analyzed using the Avrami equation. According to the Avrami model,<sup>42,43</sup> the relative degree of crystallinity  $X_{\text{rel}}$  is described as follows:

$$X_{\text{rel}}(t) = 1 - \exp(-kt^n) \quad (3)$$

where  $n$  is the Avrami exponent that depends on the nature of the nucleation mechanism and growth geometry of crystals,  $k$  is the crystallization rate constant that involves both nucleation and growth rate parameters, and  $t$  is time.

Equation (3) can be transformed into the double-logarithmic form,

$$\log[-\ln(1 - X_{\text{rel}}(t))] = \log k + n \log t \quad (4)$$

The parameters  $n$  (slope) and  $k$  (intercept) were determined by plotting  $\log\{-\ln[1 - X_{\text{rel}}(t)]\}$  against  $\log t$ . The crystallization half time  $t_{1/2}$  (i.e.,  $X_{\text{rel}} = 0.5$ ) was computed as follows:

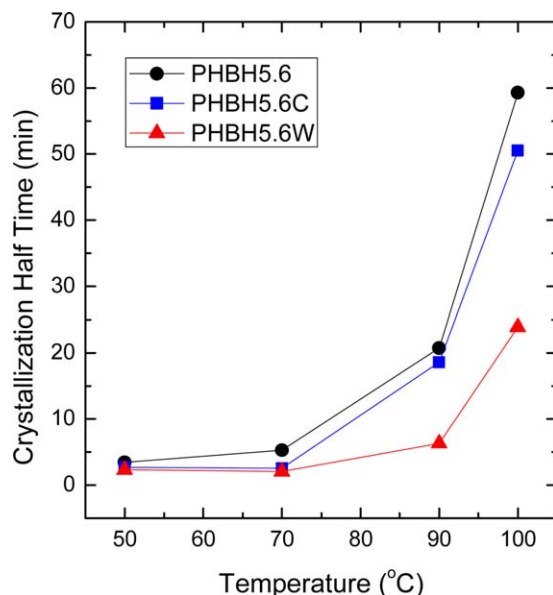
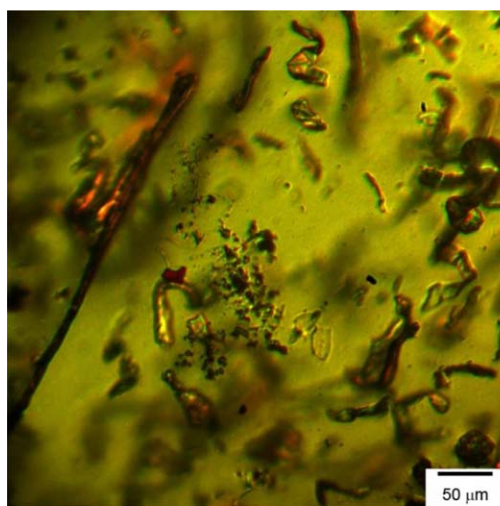


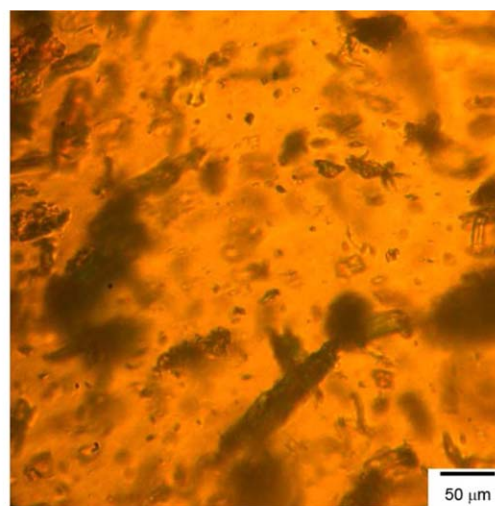
**Figure 5.** Crystallization half time of PHBH5.6-based materials versus isothermal crystallization temperature. [Color figure can be viewed in the online issue, which is available at wileyonlinelibrary.com.]

$$t_{1/2} = \left( \frac{\ln 2}{k} \right)^{\frac{1}{n}} \quad (5)$$

The Avrami double-logarithmic plots are shown in Figure 4 [with isothermal crystallization temperature being 50 °C in Figure 4(a), 70 °C in Figure 4(b), 90 °C in Figure 4(c), and 100 °C in Figure 4(d)]. At each isothermal crystallization temperature, PHBH5.6, PHBH5.6C, and PHBH5.6W exhibited almost linear and parallel lines, which suggests that  $n$  values of the three materials are similar; that is, the three materials have similar nucleation mechanism and growth geometry. Also, the lines in the figure, from left to right, are located in the order of PHBH5.6W, then PHBH5.6C, and then PHBH5.6, which



(a)



(b)

**Figure 6.** Polarized optical micrographs of PHBH5.6 with (a) cellulose flour and (b) wood flour at 190 °C. [Color figure can be viewed in the online issue, which is available at wileyonlinelibrary.com.]

**Table VI.** Linear Radius Growth Rate and Nucleation Density for PHBH5.6-Based Materials

Temperature (°C)	Material	$G$ ( $\mu\text{m}/\text{min}$ )	$N$ ( $/\text{mm}^3$ )
70	PHBH5.6	0.46 (0.01)	$1.7 \times 10^{-2}$
	PHBH5.6C	0.40 (0.01)	$3.0 \times 10^{-1}$
	PHBH5.6W	0.38 (0.01)	$5.7 \times 10^{-1}$
90	PHBH5.6	0.40 (0.01)	$8.1 \times 10^{-4}$
	PHBH5.6C	0.39 (0.03)	$1.2 \times 10^{-3}$
	PHBH5.6W	0.30 (0.02)	$3.5 \times 10^{-2}$

The numbers in the parenthesis are the standard deviations ( $n = 3$ ).

indicates that the  $k$  (crystallization rate constant) values are ranked in the following order: PHBH5.6W > PHBH5.6C > PHBH5.6. Avrami parameters calculated from the plots in Figure 4 are sum-

marized in Table IV. Avrami exponent  $n$  is in the range of 2.28 to 2.94 and showed no particular trend for material type and isothermal crystallization temperature. On the other hand, crystallization rate constant  $k$  of neat PHBH5.6 decreased with the increase of isothermal crystallization temperature, but  $k$  values of PHBH5.6C and PHBH5.6W increased with the increase of isothermal crystallization temperature from 50 to 70 °C, and decreased with the further increase of temperature. This is likely due to the changeover from viscosity/transport limited crystallization to growth rate limited crystallization.

Figure 5 depicts the crystallization half time of PHBH5.6, PHBH5.6C, and PHBH5.6W as a function of isothermal crystallization temperature. The addition of natural flours decreased the crystallization half time of neat PHBH5.6, and the wood flour-containing composite had the shortest crystallization half time at each isothermal crystallization temperature. Additionally, isothermal

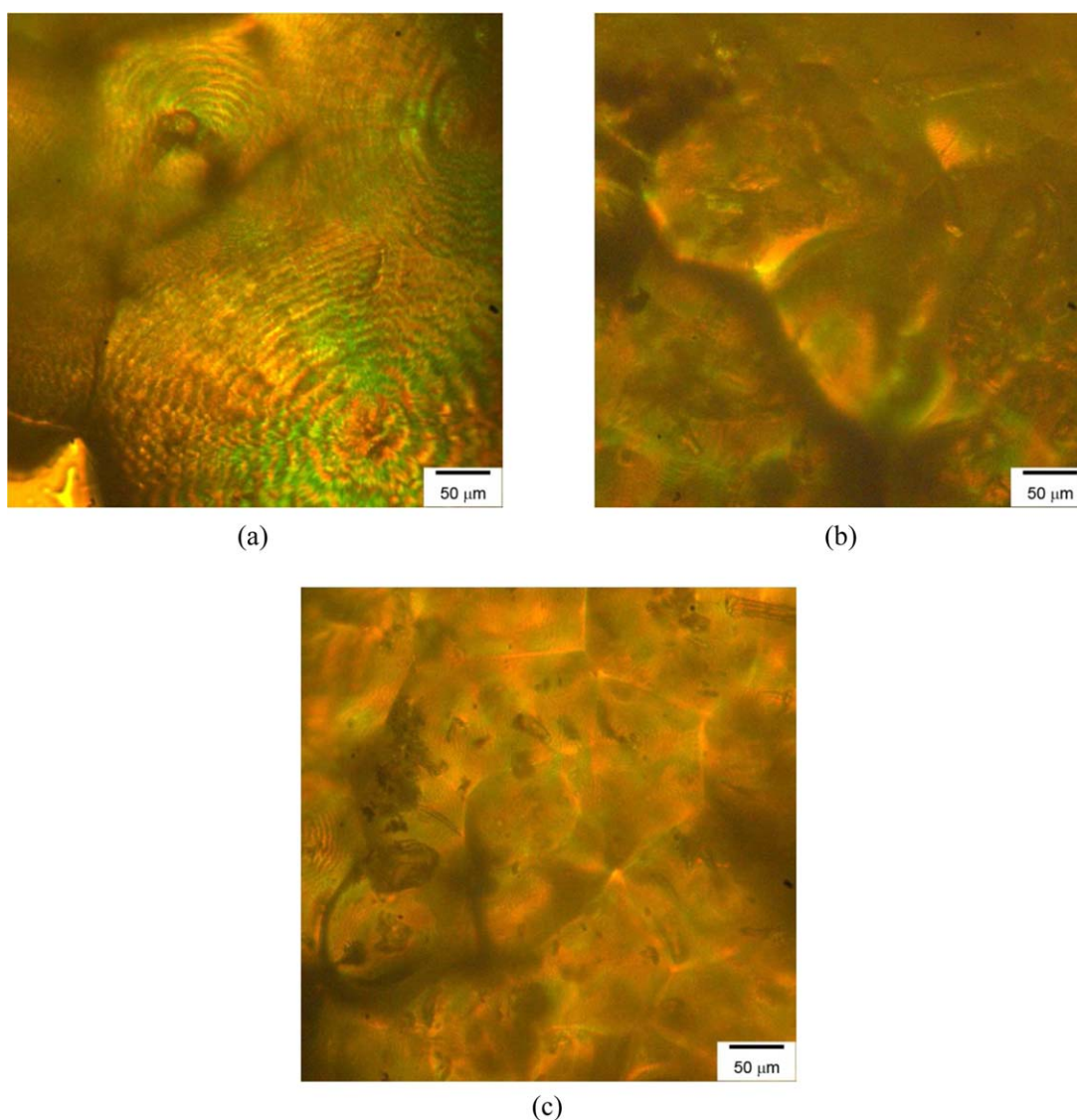


**Figure 7.** Polarized optical micrographs of (a) PHBH5.6, (b) PHBH5.6C, and (c) PHBH5.6W at isothermal crystallization temperature of 70 °C. [Color figure can be viewed in the online issue, which is available at [wileyonlinelibrary.com](http://wileyonlinelibrary.com).]



crystallization temperature affected the crystallization half time of each material differently: crystallization half time of neat PHBH5.6 increased with the increase of isothermal crystallization temperature; crystallization half time of PHBH5.6 with cellulose flour little changed from 50 to 70 °C (being 2.69 and 2.55 min, respectively), and increased with the further increase of temperature; and crystallization half time of PHBH5.6 with wood flour slightly decreased from 50 to 70 °C (being 2.32 and 2.07 min, respectively), and increased when subjected to temperatures greater than 70 °C.

### Morphology of Spherulite

Figure 6 shows polarized optical micrographs of PHBH5.6 with cellulose flour [Figure 6(a)] and wood flour [Figure 6(b)] at 190 °C (before the isothermal experiment). The figure suggests that cellulose flour has higher aspect ratio. The figure also shows that both cellulose and wood flour dispersed well in PHBH5.6 and extensive agglomeration of the natural flours was not observed. Lengths and widths of cellulose and wood flours (100 flours each) were measured from optical micrographs. The results, which are summarized in Table VI, indicate that the cellulose and wood flours have similar length, but the wood flour has larger width as well as larger amount of variation in length and width than the cellulose flour.

Figure 7 demonstrates polarized optical micrographs of PHBH5.6 [Figure 7(a)], PHBH5.6C [Figure 7(b)], and PHBH5.6W [Figure 7(c)] after complete crystallization at the isothermal temperature of 70 °C. The addition of natural flours generated smaller and more spherulites; spherulite size has the following ranked order: PHBH5.6 > PHBH5.6C > PHBH5.6W. Figure 8 illustrates spherulite radius  $R$  of PHBH5.6, PHBH5.6C, and PHBH5.6W as a function of time at the isothermal crystallization temperature of 70 °C [Figure 8(a)] and 90 °C [Figure 8(b)]. PHBH5.6, PHBH5.6C, and PHBH5.6W exhibited almost constant slopes. Spherulite linear radius growth rates  $G$  for the three materials were obtained from the slopes of the lines in Figure 8. The  $G$  values are summarized in Table VI. The addition of natural flours slightly decreased spherulitic growth rate in PHBH5.6, and PHBH with wood flour had the lowest  $G$  value. In addition,  $G$  value of each material decreased with the increase of isothermal crystallization temperature.

Nucleation density  $N$  in isothermal crystallization was estimated according to a model assuming simultaneous crystal nucleation and three-dimensional spherulitic growth as follows<sup>44</sup>:

$$N = \frac{3k}{4\pi G^3} \quad (6)$$

where  $k$  is the Avrami crystallization rate constant and  $G$  is the spherulite linear radius growth rate.

The  $N$  values are summarized in Table VI. The nucleation density of the three materials decreased with the increase of isothermal crystallization temperature, but PHBH5.6 with wood flour showed the highest nucleation density at each temperature. It should be noted that addition of wood flour was more effective at increasing nucleation density of PHBH5.6 with higher temperature.

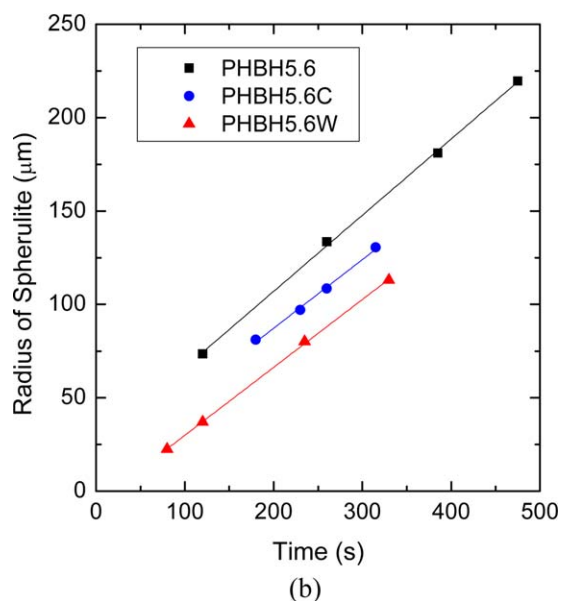
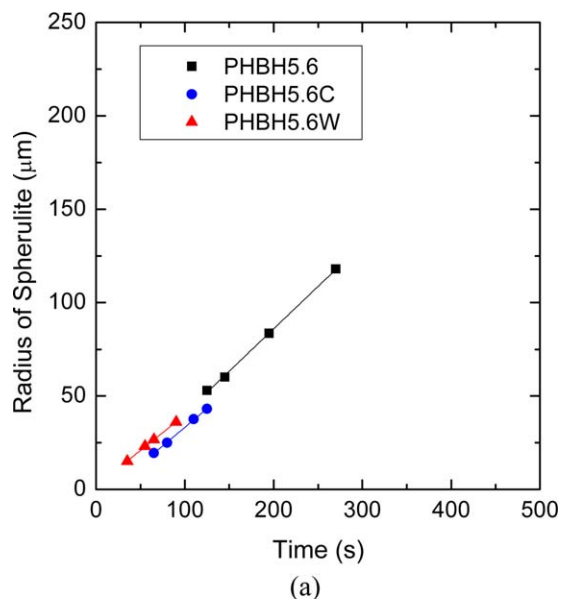


**Figure 8.** Radius of spherulite of PHBH5.6-based materials versus isothermal crystallization temperature of (a) 70 and (b) 90 °C. [Color figure can be viewed in the online issue, which is available at [wileyonlinelibrary.com](http://wileyonlinelibrary.com).]

The DSC and POM results suggested that both cellulose flour and wood flour addition enhanced the crystal nucleation in PHBH5.6, but wood flour has a higher nucleating ability than cellulose flour. The nucleating ability of cellulose and wood flour is affected by various factors. It is known that size and dispersion of a nucleating agent in the polymer matrix influence nucleation density. In general, a small and/or well-dispersed particle in the polymer matrix tends to generate small, well-dispersed crystals.<sup>45</sup> However, as shown in Figure 6 and Table VI, it is not clear whether different size and dispersion in PHBH5.6 of cellulose and wood flour was the main factor

affecting their nucleation ability. Other factors that may have influenced crystal nucleation are the surface geometry (i.e., roughness and molecular arrangement) of cellulose and wood flour, as well as bonds such as hydrogen bonds between PHBH and cellulose or wood flour. Further study is required to examine the nucleation mechanisms in PHBH5.6 with cellulose or wood flour.

## CONCLUSIONS

The effects of cellulose and wood flour on the crystallization of PHBH with a 3HH molar content of 5.6 and 11.1% were investigated. In nonisothermal crystallization, the addition of 1 wt % of cellulose or wood flour to PHBH5.6 increased crystallization peak temperature and (in the case of cellulose flour) greatly decreased or (in the case of wood flour) eliminated enthalpy of cold crystallization. Furthermore, both cellulose and wood flour increased the degree of crystallinity of PHBH5.6. Comparing the two natural flours, wood flour was found to have greater effects on PHBH5.6 crystallization behavior than cellulose flour. On PHBH11.1 crystallization behavior, however, addition of cellulose or wood flour had little effect. In isothermal crystallization, both cellulose and wood flour addition decreased the crystallization half time of PHBH5.6 at all temperatures applied in this study, with wood flour, due to its higher crystal nucleating ability, being more effective than cellulose flour. Crystallization half time of neat PHBH5.6 increased with the increase of isothermal crystallization temperature. In contrast, crystallization half time of PHBH5.6 with cellulose flour little changed from 50 to 70 °C, and increased with further increase of temperature; and crystallization half time of PHBH5.6 with wood flour slightly decreased from 50 to 70 °C, and increased when subjected to temperatures greater than 70 °C.

## ACKNOWLEDGMENTS

The authors are grateful to Kaneka Corporation, CreaFill Fibers Corporation and American Wood Fibers, Inc. for supplying materials.

## REFERENCES

- Steinbüchel, A.; Valentin, H. E. *FEMS Microbiol. Lett.* **1995**, *128*, 219.
- Sudesh, K.; Abe, H.; Doi, Y. *Prog. Polym. Sci.* **2000**, *25*, 1503.
- Reddy, C. S.; Ghai, R.; Kalia, V. *Bioresour. Technol.* **2003**, *87*, 137.
- Chen, G. Q. *Chem. Soc. Rev.* **2009**, *38*, 2434.
- Chanprateep, S. *J. Biosci. Bioeng.* **2010**, *110*, 621.
- Lee, S. Y. *Biotechnol. Bioeng.* **1996**, *49*, 1.
- Madison, L. L.; Huisman, G. W. *Microbiol. Mol. Biol. Rev.* **1999**, *63*, 21.
- Noda, I.; Green, P. R.; Satkowski, M. M.; Schechtman, L. A. *Biomacromolecules* **2005**, *6*, 580.
- Lenz, R. W.; Marchessault, R. H. *Biomacromolecules* **2004**, *6*, 1.
- Bluhm, T. L.; Hamer, G. K.; Marchessault, R. H.; Fyfe, C. A.; Veregin, R. P. *Macromolecules* **1986**, *19*, 2871.
- Scandola, M.; Ceccorulli, G.; Pizzoli, M.; Gazzano, M. *Macromolecules* **1992**, *25*, 1405.
- Yoshie, N.; Saito, M.; Inoue, Y. *Macromolecules* **2001**, *34*, 8953.
- Shimamura, E.; Kasuya, K.; Kobayashi, G.; Shiotani, T.; Shima, Y.; Doi, Y. *Macromolecules* **1994**, *27*, 878.
- Doi, Y.; Kitamura, S.; Abe, H. *Macromolecules* **1995**, *28*, 4822.
- Abe, H.; Doi, Y.; Aoki, H.; Akehata, T. *Macromolecules* **1998**, *31*, 1791.
- Sato, H.; Nakamura, M.; Padermshoke, A.; Yamaguchi, H.; Terauchi, H.; Ekgasit, S.; Noda, I.; Ozaki, Y. *Macromolecules* **2004**, *37*, 3763.
- He, J. D.; Cheung, M. K.; Yu, P. H.; Chen, G. Q. *J. Appl. Polym. Sci.* **2001**, *82*, 90.
- Asrar, J.; Valentin, H. E.; Berger, P. A.; Tran, M.; Padgett, S. R.; Garbow, J. R. *Biomacromolecules* **2002**, *3*, 1006.
- Alata, H.; Aoyama, T.; Inoue, Y. *Macromolecules* **2007**, *40*, 4546.
- Abe, H.; Doi, Y. *Biomacromolecules* **2001**, *3*, 133.
- Jacquel, N.; Tajima, K.; Nakamura, N.; Miyagawa, T.; Pan, P.; Inoue, Y. *J. Appl. Polym. Sci.* **2009**, *114*, 1287.
- Pan, P.; Liang, Z.; Nakamura, N.; Miyagawa, T.; Inoue, Y. *Macromol. Biosci.* **2009**, *9*, 585.
- Luo, R.; Xu, K.; Chen, G. *J. Appl. Polym. Sci.* **2008**, *110*, 2950.
- Dong, T.; Mori, T.; Aoyama, T.; Inoue, Y. *Carbohydr. Polym.* **2010**, *80*, 387.
- Yu, F.; Pan, P.; Nakamura, N.; Inoue, Y. *Macromol. Mater. Eng.* **2011**, *296*, 103.
- Pan, P.; Shan, G.; Bao, Y.; Weng, Z. *J. Appl. Polym. Sci.* **2013**, *129*, 1374.
- Zini, E.; Focarete, M. L.; Noda, I.; Scandola, M. *Compos. Sci. Technol.* **2007**, *67*, 2085.
- Hosoda, N.; Tsujimoto, T.; Uyama, H. *ACS Sustain. Chem. Eng.* **2014**, *2*, 248.
- Bledzki, A. *Prog. Polym. Sci.* **1999**, *24*, 221.
- Kuboki, T.; Lee, Y. H.; Park, C. B.; Sain, M. *Polym. Eng. Sci.* **2009**, *49*, 2179.
- Miao, C.; Hamad, W. *Cellulose* **2013**, *20*, 2221.
- Kuboki, T. *J. Cell. Plast.* **2014**, *50*, 113.
- Kuboki, T. *J. Cell. Plast.* **2014**, *50*, 129.
- Barham, P. J.; Keller, A.; Otun, E. L.; Holmes, P. A. *J. Mater. Sci.* **1984**, *19*, 2781.
- Crist, B.; Mirabella, F. M. *J. Polym. Sci. B: Polym. Phys.* **1999**, *37*, 3131.
- Organ, S. J.; Barham, P. J. *J. Mater. Sci.* **1991**, *26*, 1368.

37. Watanabe, T.; He, Y.; Fukuchi, T.; Inoue, Y. *Macromol. Biosci.* **2001**, *1*, 75.
38. Chen, C.; Cheung, M. K.; Yu, P. H. F. *Polym. Int.* **2005**, *54*, 1055.
39. Hu, Y.; Zhang, J.; Sato, H.; Noda, I.; Ozaki, Y. *Polymer* **2007**, *48*, 4777.
40. Ye, H. M.; Wang, Z.; Wang, H. H.; Chen, G. Q.; Xu, J. *Polymer* **2010**, *51*, 6037.
41. Ding, C.; Cheng, B.; Wu, Q. *J. Therm. Anal. Calorim.* **2010**, *103*, 1001.
42. Avrami, M. *J. Chem. Phys.* **1940**, *8*, 212.
43. Avrami, M. *J. Chem. Phys.* **1941**, *9*, 177.
44. Fillon, B.; Lotz, B.; Thierry, A.; Wittmann, J. C. *J. Polym. Sci. B: Polym. Phys.* **1993**, *31*, 1395.
45. Wunderlich, B. *Macromolecular Physics*; Academic Press: New York, **1973**.